

See discussions, stats, and author profiles for this publication at: <https://www.researchgate.net/publication/6931746>

Influence of the Environment on Photoinduced Electron Transfer: Comparison between Organized Monolayers at the Air–Water Interface and Monolayer Assemblies on Glass

ARTICLE *in* THE JOURNAL OF PHYSICAL CHEMISTRY B · JANUARY 2006

Impact Factor: 3.3 · DOI: 10.1021/jp0522967 · Source: PubMed

CITATIONS

2

READS

32

4 AUTHORS, INCLUDING:



M. Isabel Sáñez

University of Santiago de Compostela

33 PUBLICATIONS 400 CITATIONS

SEE PROFILE

Influence of the Environment on Photoinduced Electron Transfer: Comparison between Organized Monolayers at the Air–Water Interface and Monolayer Assemblies on Glass

I. Sáñdez-Macho,^{*,†} J. Gonzalez-López,[†] A. Suárez-Varela,[†] and D. Möbius[‡]

Department of Physical Chemistry, Faculty of Pharmacy, University of Santiago de Compostela, 15706 Santiago de Compostela, Spain, and Abteilung NanoBiophotonik, Max-Planck-Institut für biophysikalische Chemie, D-37070 Göttingen, Germany

Received: May 3, 2005; In Final Form: September 12, 2005

Photoinduced electron transfer (PET) has been investigated in organized monolayers at the air–water interface and in monolayer assemblies on glass in an effort to evaluate the influence of solvent reorganization and molecular dynamics on PET. The donor monolayer contained an amphiphilic thiacyanine dye, and the electron acceptors were methyl viologen and dioctadecyl viologen, respectively. The distance dependence is described here by a hard disk model, where an acceptor molecule within a disk with a radius r_{DA} around the excited donor molecule quenches the donor fluorescence due to electron transfer. Acceptor molecules outside the disk are considered ineffective. The critical radius r_{DA} is larger in monolayer assemblies on glass ($r_{\text{DA}} = 1.97$ nm) than at the air–water interface ($r_{\text{DA}} = 1.15$ nm) as evaluated from steady-state fluorescence quenching. This large difference indicates that the time between thermal collisions generating and destroying the energetic match required for electron tunneling from the excited donor molecule to the acceptor is quite different in the two systems that are compared.

Introduction

Photoinduced electron transfer (PET) phenomena have been extensively investigated in microheterogeneous environments, such as micelles, vesicles, and microemulsions.¹ Recently, charge transfer on the nanoscale has been reviewed.² These studies have revealed the important role of interfaces in enhancing the efficiency of photochemical processes. The investigation of PET in monolayers assemblies and organized monolayers at the air–water interface is particularly attractive since these systems may be considered rigid structures of specially designed architecture.³ An important advantage of organized monolayers as compared to disperse systems in solution is the possibility to control experimentally the position and the orientation of the donor and acceptor, respectively.^{3–5} In particular, photoinduced electron transfer in monolayers at the air–water interface from an excited amphiphilic cyanine dye to the amphiphilic octadecyl viologen (OV) has been investigated by transient fluorescence measurements.⁶ In this work, we studied, in the first stage, the photoinduced electron transfer between an excited cyanine dye (*N,N'*-dioctadecylthiacyanine TC) incorporated in a matrix monolayer of dimyristoylphosphatidic acid (DMPA) and an appropriate electron acceptor [methyl viologen (MV)] dissolved in the aqueous subphase, which is adsorbed at the monolayer–water interface due to electrostatic interactions with the headgroups of the matrix. This nonamphiphilic acceptor differs from OV in that it may have an orientation different from that of OV, and it offers the possibility of escape into the bulk solution of the viologen radical formed. This radical has been used as electron

shuttle in systems for the conversion of light into chemical or electric energy.⁷ The adsorption isotherm of the acceptor MV was determined to obtain information about its surface density. This system is compared with an analogous system in monolayer assemblies on glass plates, using the same donor and the acceptor OV that is equivalent to MV. The surface density of OV is varied by incorporating it in a monolayer matrix of cadmium eicosanoate (C20) at various molar ratios. In the two systems, the mobility of molecules involved in PET as well as the molecules surrounding the donor and acceptor is different. The effect of solvent on both driving force and reorganization energy has been investigated for intramolecular PET in porphyrin dyads.⁸ In fact, the driving force due to different dielectric constants as well as solvent reorganization and molecular dynamics should differ in monolayers at the air–water interface from those in monolayer assemblies. Therefore, the average range of photoinduced electron transfer as characterized by a critical distance should be different in the two systems. For the evaluation of these differences, we used the “hard disk model”. This model, in analogy to the well-known “hard sphere” model of electron transfer in solution,⁹ is applied to this case of two-dimensional systems represented by the organized monolayer at the air–water interface and by the monolayer assemblies where the donor and acceptor are located at the same interface. An acceptor molecule within a disk with a radius r_{DA} around the excited donor molecule quenches the donor fluorescence due to electron transfer. Acceptor molecules outside the disk are considered ineffective.

Experimental Section

Materials. The molecule used as donor, 3-octadecyl-2-[(3-octadecyl-2(3*H*)-benzothiazolylidene)methyl]benzothiazolium perchlorate or *N,N'*-dioctadecylthiacyanine perchlorate (TC), was purchased from Hayashibara Biochemical Laboratories, Inc., Kankoh-Shikiso Institute, and was used as received. As accep-

* To whom correspondence should be addressed: Department of Physical Chemistry, Faculty of Pharmacy, University of Santiago de Compostela, E-15782 Santiago de Compostela, Spain. Telephone: +34-9-81563100, ext. 14916. Fax: +34-9-81594912. E-mail: qfbel@usc.es.

[†] University of Santiago de Compostela.

[‡] Max-Planck-Institut für biophysikalische Chemie.

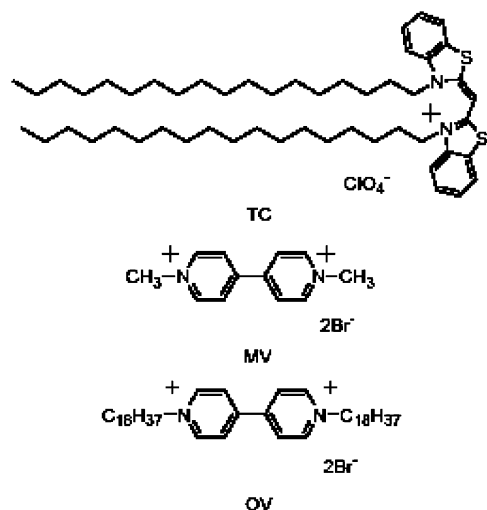


Figure 1. Chemical structures and abbreviations of active components.

tors methyl viologen bromide (MV) and *N,N'*-dioctadecyl-4,4'-bipyridinium bromide (OV) were used. The main difference between these acceptors is that the latter is amphiphilic due to the two long hydrocarbon chains. Both were obtained from Sigma-Aldrich. The chemical structures of these compounds are shown in Figure 1. The donor was selected by taking into account the fact that the emission spectrum does not overlap with the absorption spectrum of the viologen radical formed by electron transfer to MV and OV, respectively, avoiding possible energy transfer quenching of excited TC in addition to photoinduced electron transfer.

The lipid dimyristoylphosphatidic acid (DMPA) was purchased from Sigma. Eicosanoic acid, *p.a.*, obtained from Merck, was recrystallized from ethanol before use.

Preparation of Monolayers at the Air–Water Interface. Monolayers were prepared by spreading a chloroform solution of TC and a matrix of dimyristoylphosphatidic acid (DMPA) on the aqueous subphase (Millipore water, pH 5.6). A TC:DMPA molar ratio of 1:20 was used in all experiments. The solution was spread with a Microman Gilson microsyringe, precise to $\pm 0.2 \mu\text{L}$. After the solution had been spread, the monolayers were left for 10 min to ensure solvent evaporation, and afterward were compressed with a barrier speed of 15 cm²/min. Methyl viologen, used as acceptor, was dissolved in the subphase (concentration range of 10^{-8} – 10^{-5} M). The subphase temperature of 20 °C was controlled to within 0.1 °C by a thermostat. The experiments were carried out with a single-barrier NIMA 601 trough (Coventry, U.K.), with a total area of 550 cm², placed on an antivibration table. The surface pressure was measured with an accuracy of ± 0.1 mN/m using a Wilhelmy plate made from chromatography paper (Whatman Chr1) as a pressure sensor. The monolayer stability was verified by monitoring the change in surface pressure while holding the area constant.

Reflection Spectroscopy. Reflection spectra were recorded with the RefSpec spectrometer, from Nanofilm Technology (NFT). The difference in reflectivity (ΔR) between the monolayer-covered water surface and the bare water surface is determined. Fluorescence spectra were recorded with a Fluoromax-2-Jobin Yvon Spex spectrofluorimeter, described elsewhere.¹⁰ Two optical fibers (excitation fiber and emission fiber) were placed at an angle of 45° to the air–water interface, approximately 3 mm above the monolayer. A neutral density filter was placed on the bottom of the trough to minimize scattering and reflection of the exciting light. The trough was

kept in darkness during the experiments. The fluorescence spectrum for the monolayer was obtained by separately scanning the background spectrum from a clean water surface and the spectrum in the presence of the monolayer, and subtracting the background from the monolayer spectrum.

Monolayers on Solid Substrates. Transfer of the monolayer onto transparent hydrophilic glass plates was done by vertical dipping at a surface pressure of 20 mN/m [monolayers of cadmium eicosanoate (C20) and mixed monolayers of OV and cadmium eicosanoate] and 30 mN/m (TC:DMPA ratio of 1:20). The monolayers were kept under constant surface pressure for 15 min before being transferred to glass plates according to the usual Langmuir–Blodgett technique by immersion and withdrawal of the plates with alternate deposition head-to-head and tail-to-tail (Y type). The subphase for preparing the monolayer assemblies was an aqueous solution of 3×10^{-4} M CdCl₂ and 5×10^{-5} M NaHCO₃. In one half of the glass plate, the monolayer of TC:DMPA molar ratio of 1:20 was covered with the mixed monolayer of OV:C20 molar ratio of 1:*n* (*n* ranging from 20 to 1000) and the other half by a monolayer of C20 serving as a reference. The difference absorption spectrum of the two sections showed that no loss of TC has occurred during the assembly procedure. The fluorescence of TC was excited under normal incidence at 405 nm, and the intensity at 480 nm was scanned across the slide under an angle of 45° to determine the relative intensity I/I_0 , where *I* refers to the section of the glass plate with OV and *I*₀ to the reference section. Absorption and difference absorption spectra were measured with a modified spectrophotometer of the type described previously.¹¹

Results and Discussion

Monolayers at the Air–Water Interface. The experimental system designed to compare photoinduced electron transfer (PET) at the air–water interface with PET in monolayer assemblies consists of a mixed monolayer of TC:DMPA molar ratio of 1:20 and the divalent cation methyl viologen (MV) adsorbed from the aqueous subphase at the negatively charged headgroups of the matrix DMPA. The reason for choosing a TC:DMPA mixing ratio of 1:20 is a compromise between a reduction in the level of formation of dye associates such as dimers (the monomer of the amphiphilic dye only is present in the case of the oxacyanine dye¹²) and the ability to still measure the absorption spectrum of dye monolayers transferred to glass plates with a reasonable signal:noise ratio. Associates may show a rate of photoinduced electron transfer different from that of dye monomer. It has been observed that the apparent efficiency of PET is enhanced as compared to monomers if the donor is organized in J-aggregates.¹³

The surface pressure–area (π –*A*) isotherm (not shown) in the presence of MV (10^{-5} M) is virtually identical to that obtained in the pure water subphase. However, the reflection signal measured at a π of 20 mN/m in the wavelength range of 250–375 nm (λ) with maximum at 270 nm increases sharply with an increase in the concentration of MV in the subphase as shown in Figure 2. This band is characteristic for MV and indicates that MV is adsorbed at the monolayer–subphase interface.

These results indicate that the adsorption of MV is mainly governed by the electrostatic interactions between the negatively charged monolayer headgroups and the dicationic acceptor, as in the case of a tetracationic water soluble porphyrin.¹⁴ It may thus be concluded that the acceptor is located in the immediate vicinity of the monolayer polar headgroups and does not

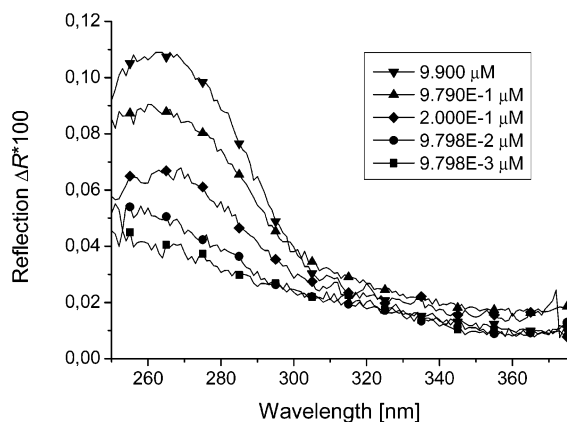


Figure 2. Reflection spectra of the 1:20 TC/DMPA monolayer at the air–water interface measured for different concentrations of MV in the subphase, with a surface pressure of 20 mN/m at 20 °C.

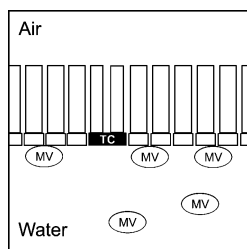


Figure 3. MV adsorbed at the polar headgroups of the matrix monolayer (schematic).

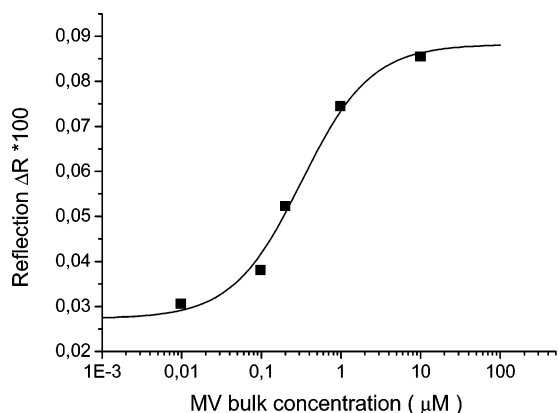


Figure 4. Reflection ΔR_{MV} plotted vs the concentration of MV in the aqueous subphase. The solid line is a least-squares fit to the Langmuir isotherm (see the text).

penetrate or intercalate in the hydrophobic region (see Figure 3). A penetration of the acceptor molecule in the monolayer should, in fact, be reflected in either a shift of the isotherm to a larger area or a change in its shape.¹⁵

The values of the reflection ΔR at 270 nm are plotted in Figure 4 versus the concentration of MV in the aqueous subphase (logarithmic scale).

These data were fitted with a Langmuir isotherm

$$\Delta R = \Delta R_0 + \frac{bx}{c + x} \quad (1)$$

where ΔR_0 at 270 nm is the reflection of the monolayer of TC:DMPA molar ratio of 1:20 on pure water, x is the concentration of MV in the aqueous subphase, and b and c are the typical parameters of the system, which characterize the equilibrium constant and the ratio between the volume concentration and the number of moles adsorbed. The least-squares

fit of eq 1 to the experimental data is shown in Figure 4 as a solid line. The following parameters are obtained from this fit: $\Delta R_0 = (0.2733 \pm 0.033) \times 10^{-3}$, $b = (0.609 \pm 0.040) \times 10^{-3}$, and $c = (3.202 \pm 0.847) \times 10^{-7}$ mol/L, with a correlation coefficient of 0.9913.

The value of the reflection at 270 nm due to the adsorption of MV is given by

$$\Delta R_{MV} = \Delta R - \Delta R_0 \quad (2)$$

$$\Delta R_{MV} = \frac{bx}{c + x} \quad (3)$$

This equation describes the relation between the concentration of MV in the aqueous subphase and MV adsorbed at the DMPA monolayer.

The reflection ΔR_{MV} is proportional to the surface density σ of MV in the case of weakly reflecting monolayers¹⁶ and can be expressed as¹⁴

$$\Delta R_{MV} = 2.303 f_{\text{orient}} \left(\frac{\epsilon}{\text{L mol}^{-1} \text{ cm}^{-1}} \right) \times 1.66 \times 10^{-7} \left(\frac{\sigma}{\text{nm}^{-2}} \right) \sqrt{R_i} \quad (4)$$

where f_{orient} is a numerical factor that takes into account the different orientation of the transition moments in solution as compared to the monolayer at the air–water interface and the value of the reflection coefficient of the air–water interface $\sqrt{R_i} \approx 0.14$. In the case of statistical orientation of the transition moments in the monolayer plane, $f_{\text{orient}} = 1.5$. If the transition moments are tilted, f_{orient} is smaller, approaching 0 for an orientation normal to the monolayer plane. The extinction coefficient (ϵ) of MV at 270 nm in the aqueous solution equals 20 700 L mol^{−1} cm^{−1}. Then

$$\Delta R_{MV} = 1.6618 \times 10^{-3} \times \left(\frac{\sigma}{\text{nm}^{-2}} \right) \quad (5)$$

Assuming the same extinction coefficient for OV, the ΔR_{OV} value of 0.71×10^{-3} calculated according to eq 5 for a 1:10 OV/C20 monolayer ($\sigma = 0.426 \text{ nm}^{-2}$) is in good agreement with the observed value of 0.8×10^{-3} (spectrum not shown), indicating a statistical orientation of the transition moments of OV in the monolayer plane. Since the orientation of adsorbed MV is not known, eq 5 may not be able to be applied to determine the surface density of MV. Therefore, we write

$$\left(\frac{\sigma}{\text{nm}^{-2}} \right) = \frac{b'x}{c + x} \quad (6)$$

The fluorescence of the cyanine dye TC is quenched in the presence of adsorbed MV due to photoinduced electron transfer. Figure 5 shows the emission spectra of the 1:20 TC/DMPA mixed monolayer on the aqueous subphase with different concentrations of MV.

Figure 6 shows the plot of the relative fluorescence intensity I/I_0 at the maximum ($\lambda_{\text{max}} = 470 \text{ nm}$) versus the bulk concentration of MV, where I_0 is the intensity of TC (excited donor) in the absence and I in the presence of MV. The concentrations of MV and the values of the relative fluorescence intensity are listed in Table 1.

According to the hard disk model, the relative fluorescence intensity I/I_0 is given by the probability of not having an acceptor molecule in the disk with a radius r_{DA} around the excited

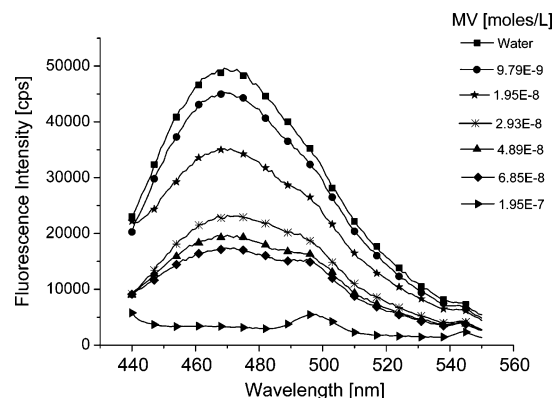


Figure 5. Fluorescence spectra of 1:20 TC/DMPA monolayers on aqueous subphases with different concentrations of MV, with excitation at 428 nm and a surface pressure of 20 mN/m at 20 °C.

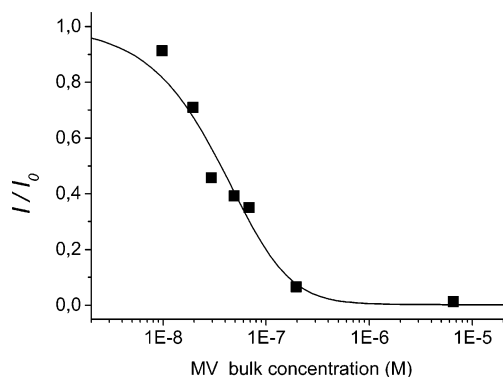


Figure 6. Relative donor fluorescence I/I_0 (I in the presence of MV in the subphase and I_0 in the absence of MV) plotted vs the bulk concentration of MV. The solid line is a least-squares fit to eq 11 based on the hard disk model of photoinduced electron transfer.

TABLE 1: Surface Densities of Methyl Viologen (MV), Adsorbed at the Organized 1:20 TC/DMPA Monolayer from the Aqueous Subphase at Different Bulk Concentrations of MV, and Relative Fluorescence Intensities I/I_0 of TC with a Surface Pressure of 20 mN/m at 20 °C

MV concentration (mol/L)	surface density (nm ⁻²)	I/I_0
9.79×10^{-9}	0.05	0.91
1.95×10^{-8}	0.01	0.71
2.93×10^{-8}	0.14	0.46
4.89×10^{-8}	0.23	0.39
6.85×10^{-8}	0.30	0.35
1.95×10^{-7}	0.65	0.07

molecule of TC. We consider an area A with one excited donor molecule and N acceptor molecules. The probability that no acceptor molecule is present in this disk is

$$p_1 = 1 - \pi r_{\text{DA}}^2 / A \quad (7)$$

and the probability of having none of the N acceptor molecules in the disk is therefore

$$\rho_N = (1 - \pi r_{\text{DA}}^2 / A)^N \quad (8)$$

The acceptor density σ_A equals N/A . Equation 8 is rewritten as

$$\rho_N = \left(1 - \frac{\pi r_{\text{DA}}^2}{A}\right)^{(\pi r_{\text{DA}}^2 \sigma_A A) / (\pi r_{\text{DA}}^2)} \quad (9)$$

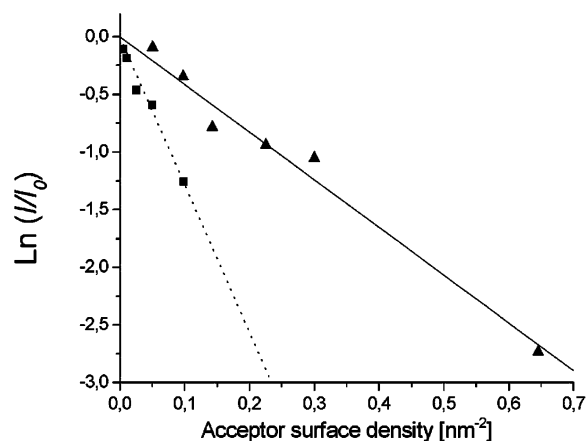


Figure 7. Logarithmic plot of the relative donor fluorescence intensity I/I_0 vs acceptor surface density: (▲) TC/MV system and (■) OV/TC system. Straight lines are least-squares fits according to eq 10.

In the limit $A \rightarrow \infty$, the probability ρ_N is equal to the ratio I/I_0 and

$$\frac{I}{I_0} = \exp(-\pi r_{\text{DA}}^2 \sigma_A) \quad (10)$$

According to eq 10, which describes the hard disk model, the relative donor fluorescence intensity I/I_0 decreases exponentially with an increase in the acceptor surface density.

To determine the critical radius r_{DA} corresponding to the hard disk using eq 10, we introduce the surface density σ of MV according to eq 6 into eq 10:

$$\frac{I}{I_0} = \exp\left[-\pi r_{\text{DA}}^2 \left(\frac{b'x}{c+x}\right)\right] \quad (11)$$

The least-squares fit of eq 11 to the experimental data (taking the value of $c = 3.202 \times 10^{-7}$ mol L⁻¹ from the fit to the MV adsorption data) is shown in Figure 6 as a solid line. The following parameters are obtained: $r_{\text{DA}} = 1.122 \pm 0.035$ nm and $b' = 1.719 \pm 0.109$. The values of the surface density of MV calculated with a b' of 1.719 using eq 6 are also listed in Table 1. From these values and the values of ΔR_{MV} , the factor f_{orient} is determined according to eq 4 using the given value of the extinction coefficient. $f_{\text{orient}} \approx 0.345$ with the exception of the lowest concentration ($f_{\text{orient}} = 0.644$), corresponding to the tilt angle θ of $\approx 30^\circ$ with respect to the surface normal.¹⁷ This result appears somewhat unexpected, since MV has two positive charges that might attach the molecule to two negatively charged headgroups in a flat orientation.

As an alternative to Figure 6, the logarithm of the relative fluorescence intensity I/I_0 may be plotted versus the acceptor surface density as shown in Figure 7 (▲).

The solid line represents a linear regression through the origin with a correlation coefficient of 0.989.

From the slope, a critical radius r_{DA} of 1.15 ± 0.04 nm is obtained, which is reasonable in comparison with the results for a similar system.^{6,18}

Monolayers on Solid Substrates. The second system, to obtain information about the influence of the environment on PET by comparison with monolayers at the air–water interface, consists of monolayer assemblies on glass plates with the donor and acceptor located at the same interface. The assemblies are prepared by sequential transfer of organized monolayers from the air–water interface to the solid by the Langmuir–Blodgett technique. The same mixed 1:20 TC/DMPA monolayer as in

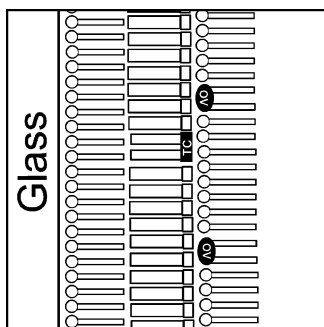


Figure 8. Monolayer assemblies on glass with donor TC and acceptor OV incorporated in different matrices and located at the same interface (schematic).

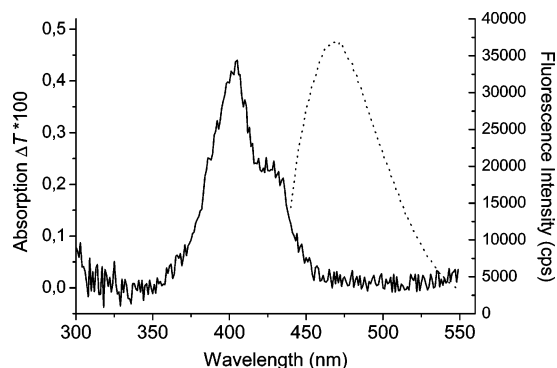


Figure 9. Absorption (ΔT , solid line) and emission (dotted line) spectra of a single monolayer of TC and DMPA in the absence of the electron acceptor OV in monolayer assemblies on glass.

the investigation at the air–water interface has been used. The acceptor, OV, which is the amphiphilic analogue of MV, was incorporated in a monolayer matrix of cadmium eicosanoate (C20) in varying 1: n OV:C20 ratios, with n ranging from 20 to 1000. Figure 8 shows schematically the structure of the monolayer assemblies.

One fundamental problem of two-component monolayers is the miscibility of the components. A criterion for mixing is the deviation of the π – A isotherm of the two-component monolayers from the isotherm calculated by superposition of the component isotherms according to their molar fractions (additivity). Such a deviation has been observed in the cases of both TC/DMPA and OV/C20 monolayers. Nevertheless, dimers of the cyanine dye TC have been observed besides dye monomers in the case of a 1:20 TC:DMPA ratio. Figure 9 shows the absorption (solid line) and emission (dotted line) spectra of an assembly with this monolayer. The absorption is plotted here as the difference ΔT in transmission between the reference section of the glass plate without dye and the section with dye. The band with a maximum at 405 nm is attributed to the dimer and the band at 430 nm to the monomer of TC.

The relative fluorescence intensity of the donor, I/I_0 , has been measured by scanning the fluorescence across glass plates with a reference section (no acceptor OV) and the sample section with a 1: n OV:C20 ratio. The surface density of OV in the mixed monolayers is calculated according to

$$\sigma = 1(n \times 0.195 \text{ nm}^2 + 0.4 \text{ nm}^2) \quad (12)$$

with values of 0.195 nm² for the area per C20 and 0.4 nm² for the area required by OV in the mixed monolayers (corresponding to the cross section of two hydrocarbon chains standing upright).

The experimental values of I/I_0 of monolayer assemblies are shown in Figure 7 (■). The straight line (dashed line) is the

least-squares fit through the origin (correlation coefficient of 0.98) corresponding to eq 10 (hard disk model). This fit has a much steeper slope than the straight line fit (solid line) of the data in the TC/MV system at the air–water interface. Consequently, the critical radius obtained from the slope ($r_{\text{DA}} = 1.97 \pm 0.07$ nm) is much larger than the critical radius ($r_{\text{DA}} = 1.15$ nm) for the air–water interface. This indicates a much larger rate of PET in the monolayer assemblies on glass plates than in organized monolayers at the air–water interface.

The different environment of donor and acceptor molecules in these two systems, TC/MV and TC/OV, may affect the photoinduced electron transfer in various ways: (1) different free enthalpy of charge separation (“driving force”), (2) different solvent reorganization and medium effects on electronic coupling of donor and acceptor, and (3) different relaxation time of thermal collisions that generate and destroy the energetic match of the electron-donating orbital and electron-accepting orbital required for electron tunneling.

The free enthalpy of charge separation, i.e., radical ion pair formation, depends on the local dielectric constant ϵ_{loc} in solution.^{8,19} Although there is no available direct information about ϵ_{loc} (at the air–water interface, an ϵ_{aw} value of ≈ 10 has been used, and an ϵ_{ma} value of ≈ 2.5 is usually taken for monolayer assemblies), it seems reasonable to assume that $\epsilon_{\text{TC/MV}} > \epsilon_{\text{TC/OV}}$, and consequently, the free enthalpy is more negative for the TC/MV system than for the TC/OV system. Therefore, due to the effect of the dielectric constant on the free enthalpy, the critical radius r_{DA} should be larger for the TC/MV system than for the TC/OV system in contrast to the observation.

The environment of the donor and acceptor may influence PET via solvent reorganization. According to the theory of nonadiabatic electron transfer, the reorganization energy is involved in expressions for both the energetic term and the electronic coupling term.^{20,21} In the energetic term, a larger reorganization energy as expected for the TC/MV system at the air–water interface as compared to the TC/OV system should lead to a larger value of r_{DA} , again in contrast to the observation.

A different approach may be considered here that has been developed to describe electron transfer in organized assemblies²² that are fundamentally different from solution phases for which the Marcus theory has been conceived. The basic idea is that electron transfer in monolayer assemblies as well as in the photosynthetic structures²³ occurs via tunneling. The rate of electron transfer (k_{DA}), therefore, is described by

$$k_{\text{DA}} = \text{const} \times \exp(-ar) \quad (13)$$

where a is the damping constant and r the distance between the donor and acceptor. In monolayer assemblies with the donor and acceptor arranged at different interfaces that were separated by fatty acid monolayers, the exponential dependence according to eq 13 has been observed with a cyanine dye as the donor, and an a of 4.1 nm^{−1} and a const. of 10¹³ s^{−1} (assuming a lifetime of the excited state of the donor in the absence of the acceptor of 10^{−9} s) were found.²² The rate of tunneling depends on the interaction energy β between the excited donor and acceptor (perturbation of the electron in the excited state of the donor by the acceptor). The interaction energy decreases exponentially with the distance since the tails of the wave functions decrease exponentially with r :

$$\beta \propto \exp\left(-\frac{2\pi r}{h} \sqrt{2m\phi}\right) \quad (14)$$

where h is Planck's constant, m the mass of the electron, and φ the height of the potential barrier represented by the medium between the donor and acceptor. Electron transfer occurs when energetic match between the donor and acceptor orbitals that are involved exists within the uncertainty limit during the exchange time $t_{\text{ex}} [=h/(2\pi\beta)]$. The energetic match will be destroyed by the next thermal collision. When t_{ex} is large compared to the time between thermal collisions that destroy energetic match (t_c), the rate is proportional to β^2 , and then $a = (4\pi/h)\sqrt{2m\varphi}$. This situation is normally considered. However, if β is sufficiently large, such that $t_{\text{ex}} < t_c$, the rate is proportional to β ; i.e., $a = (2\pi/h)\sqrt{2m\varphi}$. Unambiguous evidence for this situation has been found for photoinduced electron transfer in monolayer assemblies.^{22,24} We interpret the large value of the critical radius r_{DA} of 1.97 nm in the TC/OV monolayer systems here as being due to the situation in which $t_{\text{ex}} < t_c$, whereas in the case of the TC/MV systems with an r_{DA} of 1.15 nm, the usual situation in which $t_{\text{ex}} > t_c$ is given.

Conclusions

The photoinduced electron transfer (PET) from an excited donor to viologen has been investigated in two analogous systems with the same donor and viologen as the acceptor by steady-state fluorescence quenching of the donor. In one system, methyl viologen as the acceptor was adsorbed to the monolayer containing the donor in a monolayer matrix at the air–water interface. In the other system, dioctadecyl viologen was incorporated in monolayer assemblies with the donor and acceptor arranged at the same interface. PET as characterized by the critical radius according to the hard disk model is much more efficient in monolayer assemblies than at the air–water interface. This is interpreted as being due to different relaxation times of thermal collisions in the two systems creating and destroying the energetic match of electron-donating and -accepting molecular orbitals, similar to the situation encountered in photosynthetic structures.

Acknowledgment. We express our gratitude to the Xunta of Galicia for financially supporting Project PGIDIT03 PXIA20301PR awarded for the realization of this study. D.M. thanks the Fonds der Chemischen Industrie, Germany, for financial support.

References and Notes

- (1) Kalyanasundaram, K., Ed. *Photochemistry in microheterogeneous systems*; Academic Press: New York, 1988.
- (2) Adams, D. M.; Brus, L.; Chidsey, C. D. E.; Creager, S.; Creutz, C.; Kagan, C. R.; Kamat, P. V.; Lieberman, M.; Lindsay, S.; Marcus, R. A.; Metzger, R. M.; Michel-Beyerle, M. E.; Miller, J. R.; Newton, M. D.; Rolison, D. R.; Sankey, O.; Schanze, K. S.; Yardley, J.; Zhu, X. D. *J. Phys. Chem. B* **2003**, *107*, 6668–6697.
- (3) Möbius, D. *Acc. Chem. Res.* **1981**, *14*, 63–68.
- (4) Kuhn, H. Photoprocesses in Monolayer Assemblies. In *Light-Induced Charge Separation in Biology and Chemistry*; Gerischer, H., Katz, J. J., Eds.; Verlag Chemie: Weinheim, Germany, 1979; pp 151–169.
- (5) Ahuja, R. C.; Möbius, D. *Thin Solid Films* **1989**, *179*, 457–462.
- (6) Matsumoto, M.; Ahuja, R. C.; Möbius, D. *J. Phys. Chem.* **1992**, *96*, 5939–5942.
- (7) Kalyanasundaram, K.; Grätzel, M.; Pelizzetti, E. *Coord. Chem. Rev.* **1986**, *69*, 57–125.
- (8) DeGraziano, J. M.; MacPherson, A. N.; Liddell, P. A.; Noss, L.; Sumida, J. P.; Seely, G. R.; Lewis, J. E.; Moore, A. L.; Moore, T. A.; Gust, D. *New J. Chem.* **1996**, *20*, 839–851.
- (9) Frank, J.; Wawilow, S. *J. Z. Phys.* **1931**, *69*, 100.
- (10) Sández, M. I.; Gil González, A.; Suárez Varela, A. *Langmuir* **2000**, *16*, 9347–9351.
- (11) Kuhn, H.; Möbius, D.; Bücher, H. Spectroscopy of Monolayer Assemblies. In *Physical Methods of Chemistry*; Weissberger, A., Rossiter, B., Eds.; John Wiley & Sons: New York, 1972; Vol. 1, Part 3B, pp 577–702.
- (12) Caminati, G.; Ahuja, R. C.; Möbius, D. *Thin Solid Films* **1992**, *210/211*, 335–337.
- (13) Möbius, D. *Mol. Cryst. Liq. Cryst.* **1979**, *52*, 235–238.
- (14) Martín, M. T.; Prieto, I.; Camacho, L.; Möbius, D. *Langmuir* **1996**, *12*, 6554–6560.
- (15) Kozarac, Z.; Dhathathreyan, A.; Möbius, D. *Colloid Polym. Sci.* **1989**, *267*, 722–729.
- (16) Grüniger, H.; Möbius, D.; Meyer, H. *J. Chem. Phys.* **1983**, *79*, 3701–3710.
- (17) Pedrosa, J. M.; Martín Romero, M. T.; Camacho, L.; Möbius, D. *J. Phys. Chem. B* **2002**, *106*, 2583–2591.
- (18) Caminati, G.; Ahuja, R. C.; Möbius, D. *Prog. Colloid Polym. Sci.* **1992**, *89*, 218–222.
- (19) Weller, A. *Z. Phys. Chem. NF* **1982**, *133*, 93–98.
- (20) Levich, V. G. *Adv. Electrochem. Electrochem. Eng.* **1966**, *4*, 249–371.
- (21) Marcus, R. A.; Sutin, N. *Biochim. Biophys. Acta* **1985**, *811*, 265–322.
- (22) Kuhn, H.; Möbius, D. Monolayer assemblies. In *Investigations of Surfaces and Interfaces*, 2nd ed.; Rossiter, B. W., Baetzold, R. C., Eds.; John Wiley & Sons: New York, 1993; Vol. IXB, pp 375–542.
- (23) Kuhn, H. *Phys. Rev. A* **1986**, *34*, 3409–3425.
- (24) Kuhn, H. Electron transfer in organized membranes. In *Advances in Electrochemistry* (Conferences on Chemical Research, November 3–5); Robert A. Welch Foundation: Houston, 1986; pp 339–368.